https://doi.org/10.53655/joe.e8336w

Jurnal OptoElektronik

Continuous Detection of Pb(II) utilizing Chitosan-Graphene Oxide Surface Plasmon Resonance Sensors based on Ag/Au and Au/Ag/Au Nanolayers

Nur Hasiba Kamaruddin[1], Nur Hidayah Azeman[1*], Mohd Hadri Hafiz Mokhtar[1] and Ahmad Ashrif A Bakar[1**]

[1]*Department of Electrical, Electronic and Systems Engineering, Faculty of Engineering and Built Environment, Universiti Kebangsaan Malaysia, 43600 Bangi, Selangor, Malaysia.*

Corresponding author: *nhidayah.az@ukm.edu.my, **ashrif@ukm.edu.my

Keywords

Surface plasmon resonance
multi-metallic
chitosan
graphene oxide
heavy metal

Article History

Received: 1 June 2021
Accepted: 8 July 2021
Published: 15 July 2021

Abstract

This work demonstrates the effect of Ag/Au and Au/Ag/Au nanolayers on the performance of chitosan (CS)-graphene oxide (GO) surface plasmon resonance (SPR) sensors for Pb(II) ion detection. The CS-GO SPR sensors are fabricated on a bi-metallic 40 nm Ag/10 nm Au and tri-metallic 10 nm Au/40 nm Ag/10 nm Au nanolayers. The sensors are tested with Pb(II) ion solution of concentrations 0.1 to 5 ppm using SPR spectroscopy. The results show that the CS-GO SPR sensor on the bimetallic Ag/Au gives a gradual shift in SPR angle from 0.1 to 1 ppm and slightly linear from 3 to 5 ppm. Meanwhile, the CS-GO SPR sensor on the tri-metallic Au/Ag/Au nanolayers provides an extended linearity range from 1 to 5 ppm with the highest shift in SPR angle of 1.8°. Additionally, the tri-metallic CS-GO SPR sensor also exhibits the greatest SNR of 0.25 as compared to 0.15 of the one on the bi-metallic nanolayers. Thus, the studies prove that the tri-metallic Au/Ag/Au nanolayer is an effective and simple approach to improve the performance of a CS-GO SPR sensor for Pb(II) ion detection.

1. Introduction

Lead (Pb(II)) ion is a type of heavy metal that possesses toxic properties which able to harm human health and the environment [1], [2]. Therefore, there is an urgent need to develop the Pb(II) ion sensors that are rapid, highly sensitive and can be conducted on-site. In recent years, various techniques have been developed to detect Pb(II) ions. The traditional way of detecting Pb(II) ion is by using the direct titration method [3], which is tedious and time-consuming. A few years later, more advanced techniques have been introduced, such as atomic absorption spectrometry (AAS) [4], inductively coupled plasma atomic emission spectroscopy (ICP-AES) [5], and dynamic light scattering [6]. However, these techniques require sample preparation and sophisticated instruments. They also suffer from drawbacks such as inability to be conducted on-site, poor selectivity, low sensitivity, and interferences from other chemical analytes [7].

Recently, optical sensor technology has been explored widely due to its remarkable advantages in the sensing field [8]–[10]. Surface plasmon resonance (SPR) is one of such techniques with the ability to detect a small molecule [11], possesses high sensitivity [12] and a label-free detection [13]. SPR phenomenon arises when a p-polarized light couples with the surface charges at the metal and dielectric interface. This phenomenon happens at the angle of reflectance or SPR angle. Since its' discovery by Kretschmann and Otto in the late sixties [14], SPR has been exploited for applications in many fields such as chemistry, biomedical and environmental. For example, one of the SPR applications in environmental studies is heavy metal detection in drinking and groundwater.

The selectivity feature of the optical sensor can be improved through the application of the sensing material [8], [15], [16]; one of such materials is chitosan (CS). Recently, CS was applied as the sensing material in the localized SPR technique [17] and as the dielectric layer of SPR sensors [8] to detect heavy metals due to its' high affinity towards such ions. However, due to the limitation of the physicochemical properties of CS [15], graphene oxide (GO) was

added to improve the sensitivity of an SPR sensor for the same application [8], [18]. The addition of GO enhances the active sensing layer due to its' larger surface area and high π-conjugation structure. GO also acts as a protective layer to the metal layer, supporting the surface plasmon at the visible range [19]. However, the CS-GO SPR sensor, fabricated on a single metal layer, suffers from a limited linearity range even though it demonstrates high sensitivity.

Gold (Au) and silver (Ag) are two common metals that are used to fabricate an SPR sensor. Ag has a larger negative real part of permittivity than Au, hence producing an SPR curve with a sharper and narrower full-width-half-maximum (FWHM). Therefore, it is said that Ag possesses a better detection accuracy than Au [8], [20]. However, Ag is known for its' lack of stability which makes it easier to oxidize hence contaminate the sensing layer. On the other hand, Au is more stable and sensitive but produces a broader FWHM thus is less accurate than Ag. Because of this limitation, the multi-metallic layer is adopted to combine the advantages of these metals where Au is normally coated on top of Ag to act as a protective layer [18], [21]. Studies also suggest that the Ag inner layer is capable of enhancing the evanescent field at the Au-dielectric interface, which helps to boost the sensing capability [8], [22].

In this work, we demonstrate the effect of different Ag/Au nanolayers on the performance of chitosan-graphene oxide (CS-GO) SPR sensor for continuous detection of Pb(II). The metallic nanolayers are bi-metallic 40 nm Ag with 10 nm Au on top (Ag/Au) and tri-metallic 40 nm Ag sandwiched in between two nanolayers of 10 nm Au (Au/Ag/Au). The CS-GO sensors were tested in the exposure of deionized water and Pb(II) ion solution of concentrations between 0.1 and 5 ppm. The Pb(II) ion concentration is chosen based on the safe Pb(II) level in wastewater as established by the United States Environmental Protection Agency (US EPA) i.e. 5 ppm. We show that the tri-metallic Au/Ag/Au CS-GO SPR sensor exhibits an extended linearity range and produces a more significant shift in SPR angle as compared to the one on the bi-metallic Ag/Au nanolayers. In addition to that, the tri-metallic CS-GO SPR sensor also demonstrates a better SNR than the other one.

2. Materials and Methods

2.1 Preparation of Chitosan-Graphene Oxide (CS-GO) Nanocomposite

The CS-GO nanocomposite was prepared by dissolving 0.4 g chitosan (Aldrich) from shrimp shells in 50 ml of 1 % acetic acid. After 24 hours, 0.05 ml glutaraldehyde and 3 ml of 1 mg/ml graphene oxide were added into the chitosan solution. The nanocomposite was stirred for another hour then sonicated for 10 minutes to obtain a homogenous solution.

2.2 Fabrication of CS-GO SPR Sensor

The CS-GO SPR sensor was fabricated on a 24 mm × 32 mm Menzel-Glasser glass slide which has been cleaned with acetone. The 40 nm Ag layer was deposited on the glass using a K.J. Lesker PVD 75 RF magnetron sputtering machine in an argon atmosphere. The working pressure and RF power were set to 0.67 Pa and 50 W, respectively. The 10 nm Au layer was deposited using a Hitachi E-1010 ion sputtering machine with a working pressure of 10 Pa and a discharge current of 15 mA. Both metal targets are 99.99 % pure, and the depositions were conducted at room temperature. For bimetallic Ag/Au nanostructures, the 40 nm Ag was coated on the glass substrate first, followed by 10 nm Au. Meanwhile, for the tri-metallic Au/Ag/Au nanostructures, the 10 nm Au was deposited first on the glass substrate, followed by 40 nm Ag and finally covered with another 10 nm Au. The metallic deposition process of Ag/Au and Au/Ag/Au is presented in Figure 1.

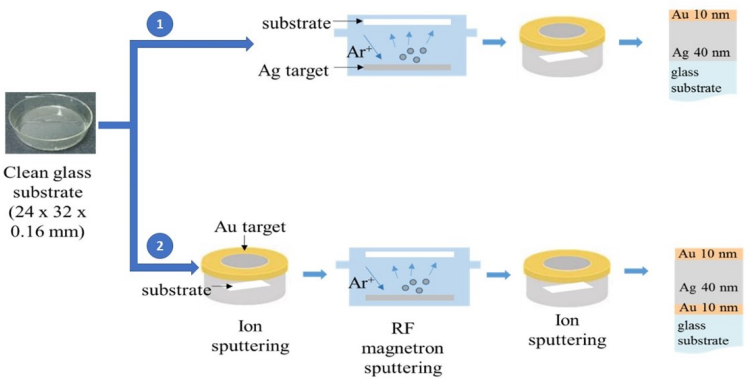

Figure 1. Metallic deposition process of Ag/Au and Au/Ag/Au

https://doi.org/10.53655/joe.e8336w

In this experiment, two CS-GO SPR sensors were prepared. The CS-GO SPR sensors were fabricated by spin-coating the CS-GO nanocomposite onto the bimetallic Ag/Au and tri-metallic Au/Ag/Au nanolayers at 6000 rpm in 30 seconds. The cross-sections of each CS-GO sensor are illustrated in Figure 2.

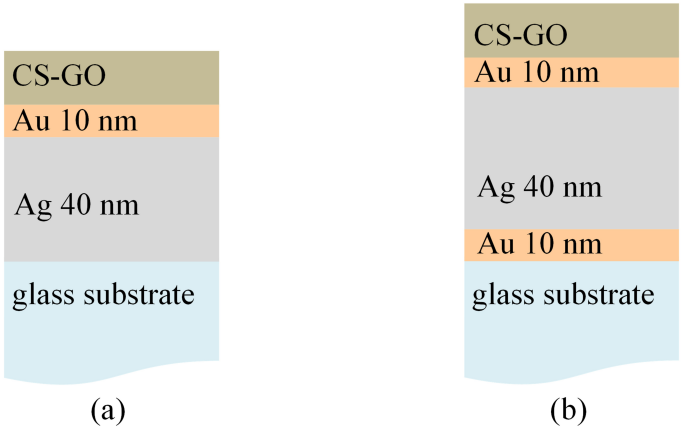

Figure 2. The CS-GO SPR sensors on (a) Ag/Au and (b) Au/Ag/Au nanolayers

The Pb(II) ion solution of concentrations 0.1 ppm, 0.5 ppm, 1 ppm, 3 ppm and 5 ppm were prepared by diluting 1000 ppm Pb(II) stock solution with deionized water. All materials used in this experiment are supplied by Sigma Aldrich (USA).

2.3 SPR Measurement System

An optical setup based on Kretschmann SPR spectroscopy was employed in this experiment. An 850 nm light was emitted from a laser diode (LD) through a collimating lens, half-wave plate, iris and polarizer to produce a p-polarized beam. The light was coupled to a BK7 prism where the CS-GO sensor was placed. The photodetector was used to measure the output power. A flow cell with a volume of approximately 2.4 ml was pressed against the CS-GO sensor to flow the analyte using a peristaltic pump where the flow rate was set at 2.0 ml/min. The SPR measurement setup is shown in Figure 3.

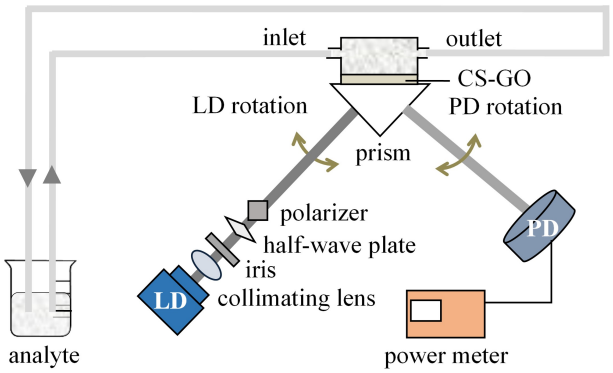

Figure 3. SPR measurement system with the CS-GO sensor placed on the prism

2.4 Procedure of Analysis

The SPR studies of each CS-GO SPR sensor was performed by first injecting the deionized water into the flow cell for 5 minutes. After 5 minutes, the p-polarized beam was modulated over an angular range of 20° - 90° to obtain the SPR reflectivity of deionized water, which will be the reference when computing the shift in SPR angle and signal-to-noise ratio (SNR) for each Pb(II) ion concentration. The affinity binding of Pb(II) ion was monitored by injecting the ion solution from concentration 0.1 to 5 ppm and recording the reflectance value at the deionized water SPR angle every 10 minutes. Each Pb(II) ion concentration was allowed to circulate through the flow cell for 30

minutes before the subsequent Pb(II) ion concentration was injected. This is to ensure that the reflectance was stable enough before determining the SPR reflectivity curve. Once the reflectance reached stability within 20 minutes after injection, the LD was re-modulated to obtain the SPR curve for that particular Pb(II) ion concentration.

3. Result and Discussion

3.1 Molecular Structure of CS-GO Nanocomposite

Raman analysis was carried out to confirm the presence of GO in CS-GO nanocomposite, and the result is presented in Figure 4. Figure 4 shows that the D band appears at around 1334 cm^{-1}, G band at approximately 1643 cm^{-1} and a broad 2D band in a range of 2778 to 3498 cm^{-1}. The shift of the bands to higher wavenumbers signifies that the sp^2 network has been perturbed by the covalent bonding between functional groups of GO and CS. The significant spread of the 2D band is related to the changes made by the grafting of CS onto the GO layers. More evident broadening in the 2D band than the D and G bands were also observed in the other studies on CS-GO nanocomposite [23], [24]. Henceforth, it is confirmed that the CS is effectively grafted onto the GO layers based on the shift of the bands, broadening of 2D band and comparable results with the previous studies [23], [24].

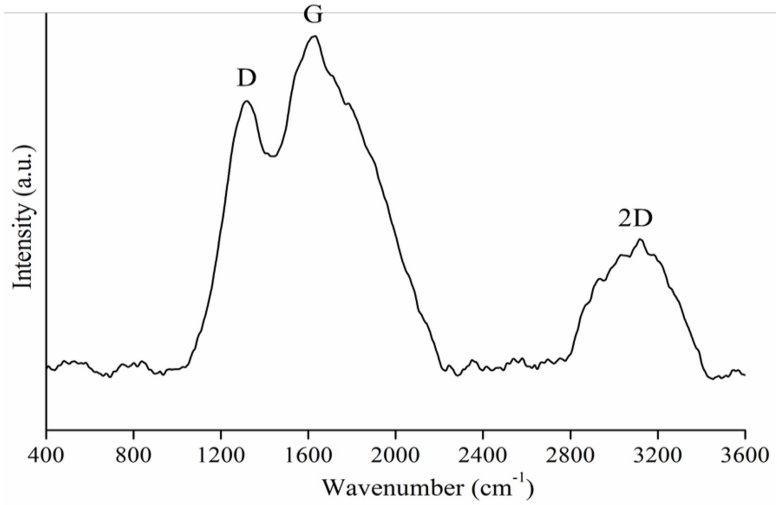

Figure 4. Raman spectra of CS-GO nanocomposite

3.2 Field Emission Scanning Electron Microscopy (FESEM) Analysis

The FESEM analysis for the bi-metallic and multi-metallic Ag/Au/CS-GO SPR sensors are shown in Figure 5. The image depicts that the bi-metallic and tri-metallic nanolayers are successfully fabricated on the glass with the required thickness. As can be seen in Figure 5(a), the uneven layer above the bi-metallic structure signifies the CS-GO nanocomposite. The surface morphology of the CS-GO layer and cross-section of the tri-metallic Au/Ag/Au/CS-GO SPR sensor has been discussed in our previous studies [18]. Likewise, other CS-GO thin film characterizations based on Atomic Force Microscopy (AFM), X-Ray Diffraction, Raman Scattering and X-Ray Photoelectron Spectroscopy (XPS) are also included therein.

3.3 Surface Plasmon Resonance Reflectivity Curve

In this work, the sensing mechanism is based on the interaction of the surface plasmon resonance field with the chemical analytes on the sensing surface of the prism. The interaction of light with metal thin film/CS-GO before and after Pb(II) ion adsorption produces a shift in the SPR angle due to a change in the refractive index. Pb(II) ion is detected based on the electrostatic interaction between the CS-GO and the Pb(II) analyte. CS can interact with Pb(II) ion due to electronegative atoms (i.e. O-H, COO-) in its structure. GO in CS structure enhanced the SPR sensitivity further due to GO's additional electronegative atoms [8].

The SPR curves of the CS-GO sensors upon exposure to deionized water (DIW) are shown in Figure 6. The SPR angles of the CS-GO sensor on the bimetallic Ag/Au and tri-metallic Au/Ag/Au are ≈81° and ≈84°. Meanwhile, the FWHMs for both are ≈5° and ≈6°, in the same order. As expected, the CS-GO SPR sensor on the bi-metallic nanolayers produces a narrower FWHM due to its' smaller thickness than the one on the tri-metallic nanolayers.

https://doi.org/10.53655/joe.e8336w

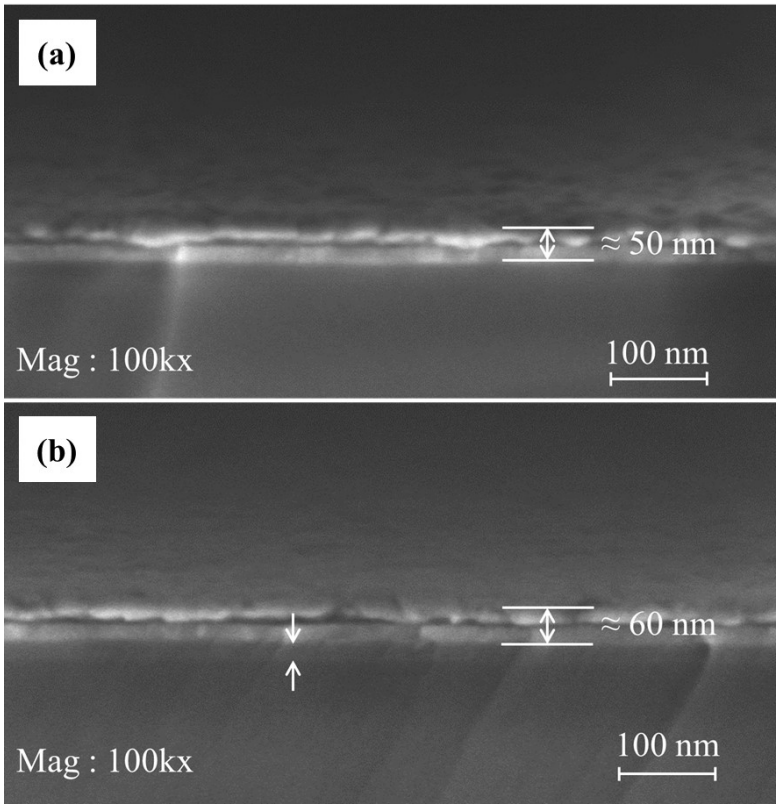

Figure 5. Cross-section of (a) bi-metallic Ag/Au/CS-GO and (b) tri-metallic Ag/Au/CS-GO SPR sensors

Note that the broader FWHM exhibited by the tri-metallic CS-GO sensor results from the increase in the total thickness of Au layer discussed in [22].

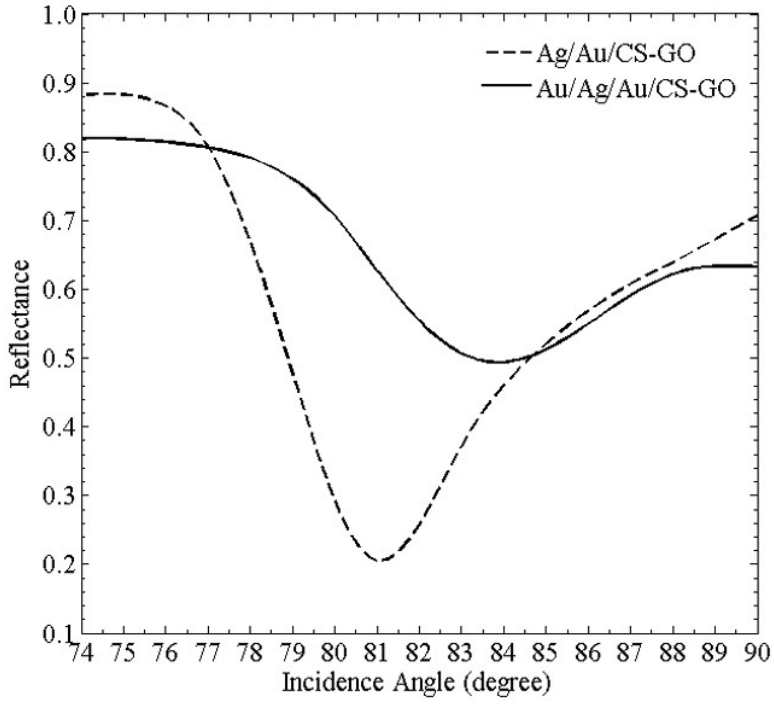

Figure 6. The SPR reflectivity curves of CS-GO SPR sensors on the bi-metallic and tri-metallic nanolayers soaked in deionized water (DIW)

3.4 Real-time Kinetics of Pb(II) Ion Binding

The ability of the sensor device to sense analyte continuously is quite appealing for a commercial sensor. In this work, the CS-GO SPR sensor was analyzed for its potential to be used under consecutive injection of the increasing Pb^{2+} ions concentration from 0.1 to 5.0 ppm. The sensorgrams in Figure 7(a) and (b) depict the real-time value of reflectance for both CS-GO sensors when measured at the SPR angle of DIW i.e. ≈81° for the Ag/Au bimetallic and ≈84° for the Au/Ag/Au tri-metallic, respectively. In Figure 7(a), the steady-state value of reflectance for 0.1, 0.5, 1.0, 3.0, and 5.0 ppm are roughly 0.22, 0.24, 0.25, 0.23 and 0.25, respectively. It is shown that the reflectance at the reference angle increases steadily as 0.1 to 1.0 ppm Pb^{2+} ion was injected into the flow cell. This infers that the binding of Pb^{2+} ions with the CS-GO nanolayer directly generated the increase in the refractive index which was manifested as a gradual increase in the reflectance. However, the reflectance drops as 3 ppm Pb^{2+} ion was mobilized then rise again when 5 ppm Pb^{2+} was circulated through the system.

Meanwhile, for Figure 7(b), the steady-state value of reflectance for 0.1 ppm, 0.5 ppm, 1 ppm, 3 ppm and 5 ppm are roughly 0.52, 0.52, 0.49, 0.52 and 0.55, respectively. The Au/Ag/Au/CS-GO SPR sensor exhibits an opposite response from the former Ag/Au/CS-GO sensors. The reflectance remains stagnant in the lower concentration range of 0.1 to 0.5 ppm but rises steadily in the higher concentration region of 1 to 5 ppm. This suggests that the Au/Ag/Au/CS-GO SPR sensor requires a higher concentration of Pb^{2+} ions to change the refractive index of the CS-GO layer thus increases the SPR reflectance. It is shown that the time taken for both the SPR signal to be stable and timely for the angular modulation at about 20 minutes which is similar to the time taken for other SPR sensors in heavy metal ion detection [25].

In Figures 7(c) and (d), the SPR reflectivity curves of both sensors show a negative shift to the left side of the DIW SPR angles. This phenomenon might be due to the leaky waves propagating in the backward direction at the metal-dielectric interface [26]. Like the forward surface wave, this backward leaky-wave can also be easily excited by a metallic thin film with negative permittivity and enhanced by the surface plasmon resonance [27]. Furthermore, the multi-metallic nanolayers that can excite multiple surface plasmon resonances also influence such shifting behaviour [28]. Nevertheless, the direction of the shifts is consistent for all measurements; hence such a response is acceptable.

3.5 Shift in SPR Angle and Linearity Range

In Figure 8, the shift in SPR angle, $\delta\theta_{SPR}$ for bi-metallic CS-GO SPR sensor increases gradually from 0.1 to 1 ppm and the $\delta\theta_{SPR}$-[Pb(II)] ion concentration relationship follows a linear model of $\delta\theta_{SPR}$ = 0.541°ppm^{-1} [Pb(II)] ppm + 0.612°. Notably, the bi-metallic CS-GO SPR sensor demonstrates a linear shift in the higher concentration region where the $\delta\theta_{SPR}$-[Pb(II)] relationship is given by $\delta\theta_{SPR}$ = 0.150°ppm^{-1} [Pb(II)] ppm + 0.450°. This can be explained by the fact that the exterior CS-GO matrix might have nearly saturated up to 1 ppm mobilization thus, the subsequent concentration of Pb(II) ion was transferred to the interior site of the matrix, which has enough available binding site [29]. Notably, the calibration curve looks like 'resetting' itself at 3 ppm when the shift goes down to 0.6° then increase again up to 0.9° at 5 ppm. Henceforth, a linear shift is observed from 3 to 5 ppm. The maximum shift in SPR angle produced by the bi-metallic Ag/Au/CS-GO SPR sensor is 1.2° which is for 5 ppm. The SPR sensitivity using bi-metallic CS-GO SPR sensor are 0.541°ppm^{-1} and 0.150°ppm^{-1} for the concentration region from 0.1 to 1 ppm and 3 to 5 ppm, respectively.

On the contrary, the tri-metallic CS-GO SPR sensor could not detect the difference between 0.1 and 0.5 ppm, yielding an equal value of $\delta\theta_{SPR}$ which is 1.2°. Nevertheless, the tri-metallic CS-GO sensor managed to detect differences in the refractive index due to the higher concentration of Pb(II) ions i.e. from 1 to 5 ppm. The shift in SPR angle elevates up to 1.8° when tested with 5 ppm, which is the highest $\delta\theta_{SPR}$ measured in this experiment. The tri-metallic Au/Ag/Au/CS-GO sensor also exhibits an extended linearity range from 1 to 5 ppm compared to 3 to 5 ppm provided by the bi-metallic CS-GO SPR sensor up to only 1 ppm by the single Au CS-GO SPR sensor [12]. The $\delta\theta_{SPR}$-[Pb(II)] relationship is given by $\delta\theta_{SPR}$ = 0.375°ppm^{-1} [Pb(II)] ppm - 0.025° and R^2 = 0.987. The SPR sensitivity using the tri-metallic CS-GO SPR sensor is 0.375°ppm^{-1} for the concentration region from 1 to 5 ppm. It is important to highlight that the results are slightly different from our previous study because the sample used in this experiment is for the whole range of concentration while the latter used one sample for each concentration. Therefore, a bigger maximum shift in SPR angle was obtained previously [18]. Nevertheless, the sample used in this study exhibits great reusability to allow Pb(II) ion binding for the whole concentrations.

Such response in the lower concentration region might be due to the thickness of the tri-metallic CS-GO sensor, which exceeds the optimal thickness of 50 nm for effective coupling [30]. Therefore, the evanescent field which penetrates the CS-GO dielectric layer might not be strong and stable enough to reach the exterior layer of the CS-GO matrix of which 0.1 to 0.5 ppm Pb(II) ions might have occupied. Due to this limitation, the tri-metallic CS-GO sensor could not detect the difference in a refractive index produced by these concentrations. However, the remarkable performance by the tri-metallic CS-GO sensor in the higher concentration region could be explained by

https://doi.org/10.53655/joe.e8336w

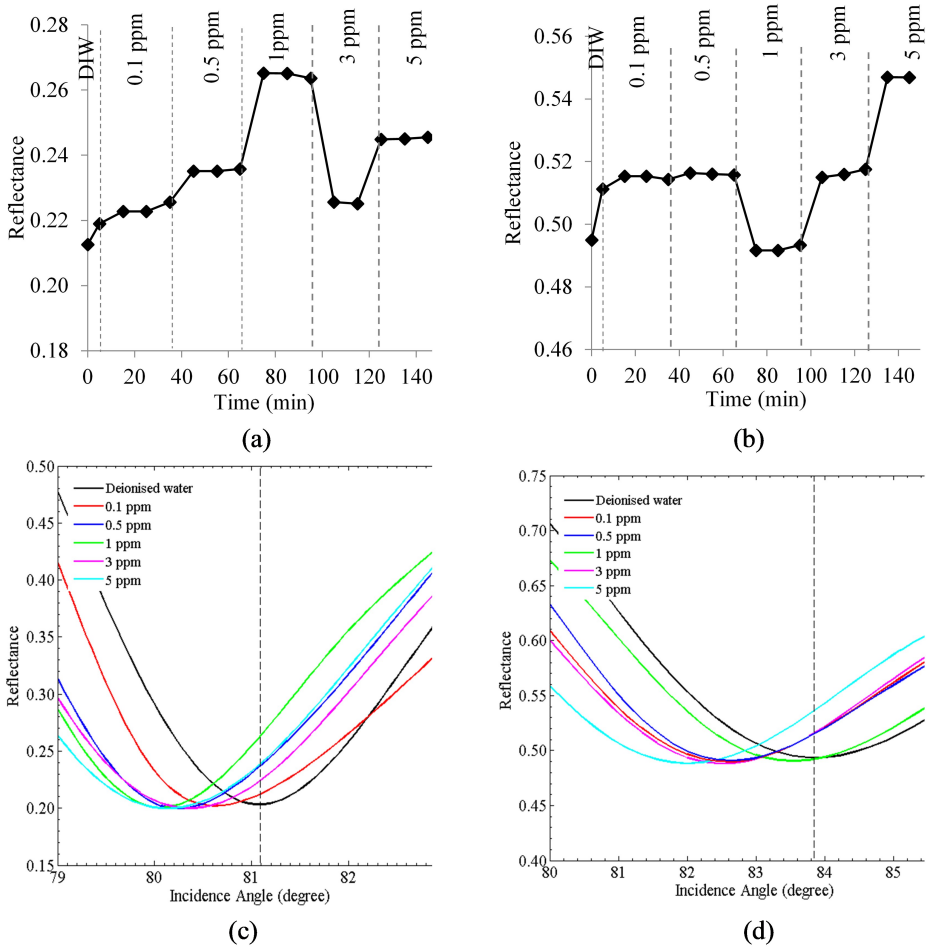

Figure 7. The sensorgram of Pb(II) ion binding with the CS-GO matrix on the (a) bi-metallic and (b) tri-metallic nanolayers measured at the SPR angles of DIW, shown by the dashed line in the reflectivity curves of both sensors (c) and (d), respectively

the fact that the Pb(II) ions might have been transferred to the interior sites of the CS-GO matrix as the exterior saturated [29]. This infers that the Pb(II) ions are now closer to the Au/CS-GO interface, whereas a stronger and more stable evanescent field exists, which enables further detection of refractive index changes [31]. Therefore, it is observed that the shift in SPR angle increases linearly from 1 to 5 ppm, thus extends the linearity range for Pb(II) ion detection. This is the attribute of the enhanced evanescent field at the interface of Au/CS-GO, which is the result of better light confinement by the Ag inner nanolayer sandwiched in between two Au nanolayers [22].

3.6 Signal-to-Noise-Ratio (SNR)

Figure 9 exhibits the signal-to-noise ratio (SNR) of bi-metallic and tri-metallic CS-GO SPR sensors. Since SNR is related to the real system measurement, each Pb(II) ion concentration will have its' own SNR value [18]. Nevertheless, considering only the highest value of SNR for each sensor, which is when tested with 5 ppm, the tri-metallic CS-GO SPR sensor yields the best SNR of 0.25 as opposed to 0.15 of the one on the bi-metallic nanolayers, as can be seen in Figure 8. The tri-metallic CS-GO SPR sensor produces the highest shift in SPR angle and the greatest SNR value. Such performance could be due to the combination of the Ag layer, which provides an acceptably narrow FWHM and two Au layers that boost the shift in SPR angle, hence yielding the best SNR. According to the results, it is proved that the tri-metallic CS-GO SPR sensor is a simple yet effective approach to improve the performance of a CS-GO SPR sensor.

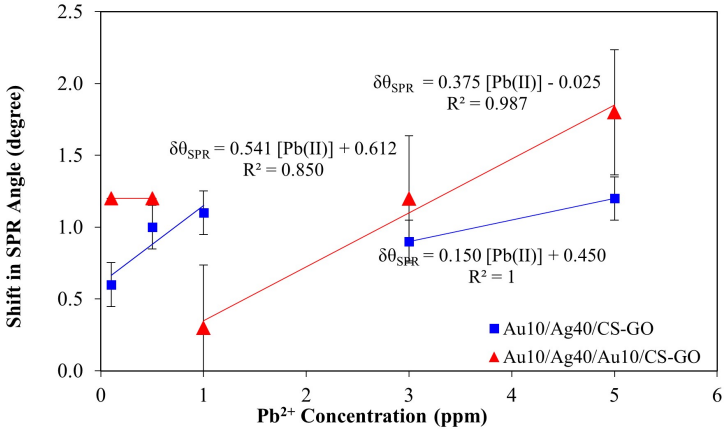

Figure 8. The shift in SPR angle and linearity range of CS-GO SPR sensor on the bi-metallic Ag/Au (blue square) and tri-metallic Au/Ag/Au (red triangle)

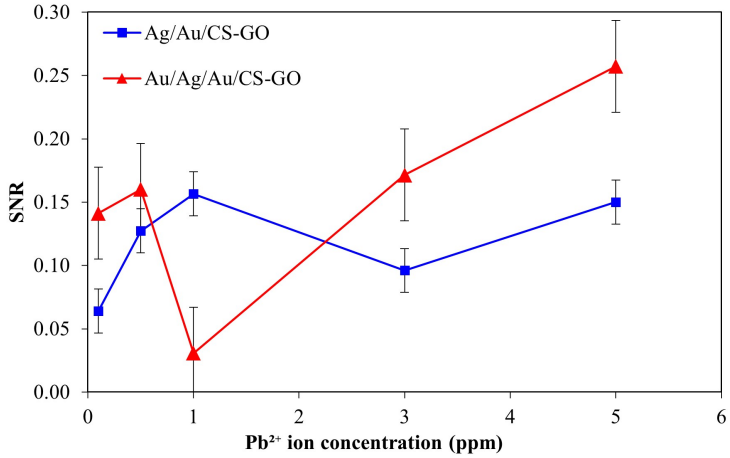

Figure 9. SNR of CS-GO SPR sensor on the bimetallic Ag/Au (blue square) and tri-metallic Au/Ag/Au (red triangle)

4. Conclusion

CS-GO SPR sensors for Pb(II) ion detection fabricated on a bi-metallic Ag/Au and tri-metallic Ag/Au/Ag nanolayers were presented. The SPR reflectivity of each CS-GO sensor was measured upon exposure to deionized water (DIW) and 0.1 to 5 ppm Pb(II) ion solutions. The CS-GO SPR sensor on the bimetallic Ag/Au nanolayers gradually changes SPR angle within the lower concentration region from 0.1 to 1 ppm and linear shift in the higher concentration region of 3 to 5 ppm. On the other hand, the CS-GO SPR sensor on the tri-metallic Au/Ag/Au nanolayers demonstrates extended linearity in the broader range of concentration from 1 to 5 ppm. The maximum SPR angle shift of the tri-metallic CS-GO sensor is 1.8°, where the one on the bi-metallic nanolayers gives 1.2°. Apart from that, the tri-metallic CS-GO SPR sensor yields the best SNR value of 0.25 compared to 0.15 of the other. Such outstanding performance of the tri-metallic CS-GO SPR sensor is the attributes of the evanescent field enhancement given by the Ag layer and improved sensitivity provided by the two Au layers. Thus, in this study, we have successfully compared the performance of CS-GO SPR sensors on the bi-metallic and tri-metallic nanolayers. The results suggested that the latter is a simple yet effective approach to boost the performance of such SPR sensor to detect heavy metal ions such as Pb(II) ions in an aqueous solution.

Conflict of Interest

The authors declare there is no conflict of interest.

https://doi.org/10.53655/joe.e8336w

Acknowledgement

The authors are grateful to the Photonics Technology Laboratory, Department of Electrical, Electronic and Systems Engineering, Faculty of Engineering and Built Environment and the Centre for Research and Instrumentation Management (CRIM), Universiti Kebangsaan Malaysia, for providing their facilities. The authors would also like to acknowledge the support of the Malaysian Ministry of Higher Education (MOHE) [Grant No: FRGS/1/2018/TK04/UKM/02/6] and Universiti Kebangsaan Malaysia [Grant No: DIP-2019-005] for funding this work. We would also like to thank MyPhD/MyBrain15 for the scholarship awarded to the first author of this paper.

References

[1] M. A. Assi, M. N. M. Hezmee, A. W. Haron, M. Y. Sabri, and M. A. Rajion, "The detrimental effects of lead on human and animal health," *Veterinary World*, vol. 9, no. 6, pp. 660–671, Jun. 2016. DOI: 10.14202/vetworld.2016.660-671.

[2] N. N. Sobihah, A. A. Zaharin, M. K. Nizam, L. L. Juen, and K. Kyoung-Woong, "Bioaccumulation of heavy metals in maricultured fish, lates calcarifer (barramudi), lutjanus campechanus (red snapper) and lutjanus griseus (grey snapper)," *Chemosphere*, vol. 197, pp. 318–324, Apr. 2018. DOI: 10.1016/j.chemosphere.2017.12.187.

[3] Z. Nan, "Determination of lead by selective chelatometric titration with HEDTA after separation as its sulphate by an improved method of precipitation," *Talanta*, vol. 37, no. 10, pp. 1021–1024, Oct. 1990. DOI: 10.1016/0039-9140(90)80144-5.

[4] M. A. Habila, E. Yilmaz, Z. A. ALOthman, and M. Soylak, "Combination of dispersive liquid-liquid microextraction and multivariate optimization for separation-enrichment of traces lead by flame atomic absorption spectrometry," *Journal of Industrial and Engineering Chemistry*, vol. 37, pp. 306–311, May 2016. DOI: 10.1016/j.jiec.2016.03.037.

[5] L. H. Yze, N. A. Yusof, N. A. M. Maamor, and N. H. Azeman, "Fabrication and characterization of molecularly imprinted polymer for hg(II) ion," *Asian Journal of Chemistry*, vol. 26, no. 16, pp. 5029–5032, 2014. DOI: 10.14233/ajchem.2014.16298.

[6] L. Zhang, Y. Yao, J. Shan, and H. Li, "Lead (II) ion detection in surface water with pM sensitivity using aza-crown-ether-modified silver nanoparticles via dynamic light scattering," *Nanotechnology*, vol. 22, no. 27, p. 275 504, May 2011. DOI: 10.1088/0957-4484/22/27/275504.

[7] D. K. Sarfo, E. L. Izake, A. P. O'Mullane, and G. A. Ayoko, "Molecular recognition and detection of pb(II) ions in water by aminobenzo-18-crown-6 immobilised onto a nanostructured SERS substrate," *Sensors and Actuators B: Chemical*, vol. 255, pp. 1945–1952, Feb. 2018. DOI: 10.1016/j.snb.2017.08.223.

[8] N. F. Lokman, N. H. Azeman, F. Suja, N. Arsad, and A. A. A. Bakar, "Sensitivity enhancement of pb(II) ion detection in rivers using SPR-based ag metallic layer coated with chitosan/graphene oxide nanocomposite," *Sensors*, vol. 19, no. 23, p. 5159, Nov. 2019. DOI: 10.3390/s19235159.

[9] G.-S. Liu, X. Xiong, S. Hu, *et al.*, "Photonic cavity enhanced high-performance surface plasmon resonance biosensor," *Photonics Research*, vol. 8, no. 4, p. 448, Mar. 2020. DOI: 10.1364/prj.382567.

[10] M. M. Elgaud, A. A. A. Bakar, A. A. Ghaith, *et al.*, "Pulse compressed time domain multiplexed fiber bragg grating sensor: A comparative study," *IEEE Access*, vol. 6, pp. 64 427–64 434, 2018. DOI: 10.1109/access.2018.2877887.

[11] F. Melaine, Y. Roupioz, and A. Buhot, "Small molecule SPR imaging detection from split aptamer microarrays," *Procedia Technology*, vol. 27, pp. 6–7, 2017. DOI: 10.1016/j.protcy.2017.04.004.

[12] N. F. Lokman, A. A. A. Bakar, F. Suja, *et al.*, "Highly sensitive SPR response of au/chitosan/graphene oxide nanostructured thin films toward pb (II) ions," *Sensors and Actuators B: Chemical*, vol. 195, pp. 459–466, May 2014. DOI: 10.1016/j.snb.2014.01.074.

[13] S. Saleviter, Y. W. Fen, W. M. E. M. M. Daniyal, J. Abdullah, A. R. Sadrolhosseini, and N. A. S. Omar, "Design and analysis of surface plasmon resonance optical sensor for determining cobalt ion based on chitosan/graphene oxide decorated quantum dots-modified gold active layer," *Optics Express*, vol. 27, no. 22, p. 32 294, Oct. 2019. DOI: 10.1364/oe.27.032294.

[14] J. Homola, S. S. Yee, and G. Gauglitz, "Surface plasmon resonance sensors: Review," *Sensors and Actuators B: Chemical*, vol. 54, no. 1-2, pp. 3–15, Jan. 1999. DOI: 10.1016/s0925-4005(98)00321-9.

[15] N. H. Azeman, N. Arsad, and A. A. A. Bakar, "Polysaccharides as the sensing material for metal ion detection-based optical sensor applications," *Sensors*, vol. 20, no. 14, p. 3924, Jul. 2020. DOI: 10.3390/s20143924.

[16] W. B. W. A. Rahman, N. H. Azeman, N. H. Kamaruddin, *et al.*, "Label-free detection of dissolved carbon dioxide utilizing multimode tapered optical fiber coated zinc oxide nanorice," *IEEE Access*, vol. 7, pp. 4538–4545, 2019. DOI: 10.1109/access.2018.2888626.

[17] S. Abdullah, N. H. Azeman, N. N. Mobarak, M. S. D. Zan, and A. A. A. Bakar, "Sensitivity enhancement of localized SPR sensor towards pb(II) ion detection using natural bio-polymer based carrageenan," *Optik*, vol. 168, pp. 784–793, Sep. 2018. DOI: 10.1016/j.ijleo.2018.05.016.

[18] N. H. Kamaruddin, A. A. A. Bakar, M. H. Yaacob, M. A. Mahdi, M. S. D. Zan, and S. Shaari, "Enhancement of chitosan-graphene oxide SPR sensor with a multi-metallic layers of au/ag/au nanostructure for lead(II) ion detection," *Applied Surface Science*, vol. 361, pp. 177–184, Jan. 2016. DOI: 10.1016/j.apsusc.2015.11.099.

[19] N.-F. Chiu, T.-Y. Huang, and H.-C. Lai, "Graphene oxide based surface plasmon resonance biosensors," in *Advances in Graphene Science*, InTech, Jul. 2013. DOI: 10.5772/56221.

[20] G. Wang, C. Wang, R. Yang, W. Liu, and S. Sun, "A sensitive and stable surface plasmon resonance sensor based on monolayer protected silver film," *Sensors*, vol. 17, no. 12, p. 2777, Nov. 2017. DOI: 10.3390/s17122777.

[21] B. A. Prabowo and K.-C. Liu, "Multi-metallic sensing layers for surface plasmon resonance sensor," in *2017 IEEE 15th Student Conference on Research and Development (SCOReD)*, IEEE, Dec. 2017. DOI: 10.1109/scored.2017.8305386.

[22] Z. Wang, Z. Cheng, V. Singh, *et al.*, "Stable and sensitive silver surface plasmon resonance imaging sensor using trilayered metallic structures," *Analytical Chemistry*, vol. 86, no. 3, pp. 1430–1436, Jan. 2014. DOI: 10.1021/ac402126k.

[23] F. Emadi, A. Amini, A. Gholami, and Y. Ghasemi, "Functionalized graphene oxide with chitosan for protein nanocarriers to protect against enzymatic cleavage and retain collagenase activity," *Scientific Reports*, vol. 7, no. 1, Feb. 2017. DOI: 10.1038/srep42258.

[24] K. Bustos-Ramírez, A. Martínez-Hernández, G. Martínez-Barrera, M. Icaza, V. Castaño, and C. Velasco-Santos, "Covalently bonded chitosan on graphene oxide via redox reaction," *Materials*, vol. 6, no. 3, pp. 911–926, Mar. 2013. DOI: 10.3390/ma6030911.

[25] M. M. Abdi, L. C. Abdullah, A. R. Sadrolhosseini, W. M. M. Yunus, M. M. Moksin, and P. M. Tahir, "Surface plasmon resonance sensing detection of mercury and lead ions based on conducting polymer composite," *PLoS ONE*, vol. 6, no. 9, M. Rini, Ed., e24578, Sep. 2011. DOI: 10.1371/journal.pone.0024578.

[26] T. Tamir, "Leaky waves in planar optical waveguides," *Nouvelle Revue d'Optique*, vol. 6, no. 5, pp. 273–284, Sep. 1975. DOI: 10.1088/0335-7368/6/5/304.

[27] X. Yin, L. Hesselink, Z. Liu, N. Fang, and X. Zhang, "Large positive and negative lateral optical beam displacements due to surface plasmon resonance," *Applied Physics Letters*, vol. 85, no. 3, pp. 372–374, Jul. 2004. DOI: 10.1063/1.1775294.

[28] P.-P. Zuo, H.-F. Feng, Z.-Z. Xu, *et al.*, "Fabrication of biocompatible and mechanically reinforced graphene oxide-chitosan nanocomposite films," *Chemistry Central Journal*, vol. 7, no. 1, Feb. 2013. DOI: 10.1186/1752-153x-7-39.

[29] A. H. Gedam, "Synthesis and characterization of graphite doped chitosan composite for batch adsorption of lead (II) ions from aqueous solution," *Advanced Materials Letters*, vol. 6, no. 1, pp. 59–67, Jan. 2015. DOI: 10.5185/amlett.2015.7592.

[30] K. N. Kudin, B. Ozbas, H. C. Schniepp, R. K. Prud'homme, I. A. Aksay, and R. Car, "Raman spectra of graphite oxide and functionalized graphene sheets," *Nano Letters*, vol. 8, no. 1, pp. 36–41, Dec. 2007. DOI: 10.1021/nl071822y.

[31] B. H. Ong, X. Yuan, S. C. Tjin, J. Zhang, and H. M. Ng, "Optimised film thickness for maximum evanescent field enhancement of a bimetallic film surface plasmon resonance biosensor," *Sensors and Actuators B: Chemical*, vol. 114, no. 2, pp. 1028–1034, Apr. 2006. DOI: 10.1016/j.snb.2005.07.064.

https://doi.org/10.53655/joe.e8336w